A LabVIEW-Based Implementation of Real-Time Adaptive Modulation for Underwater Acoustic OFDM Communication

Suchi Barua, Yue Rong, Sven Nordholm, Peng Chen
School of Electrical Engineering, Computing and Mathematical Sciences
Curtin University, Bentley, WA 6102, Australia

***Abstract*— Adaptive modulation is appealing for underwater acoustic (UA) communication systems in order to improve the system power and spectral efficiency by varying transmission parameters according to the channel condition. This paper presents a real-time orthogonal frequency-division multiplexing (OFDM) based adaptive UA communication system, implemented using the National Instruments (NI) CompactDAQ device and the LabVIEW software. A self-adapting algorithm is used to select the best modulation mode for time-varying UA channels. The signal-to-noise ratio (SNR) is calculated at the receiver and used as a performance metric to switch the modulation mode which is fed back to the transmitter for data transmission. The proposed software defined implementation is flexible and simplifies the prototype design compared to conventional digital signal processor (DSP)-based design. The experimental results verify the superiority of the adaptive transmission.**

Keywords—Adaptive modulation, time-varying channel, underwater acoustic communication, LabVIEW, CompactDAQ, orthogonal frequency-division multiplexing (OFDM).

Global Oceans 2020: Singapore - U.S. Gulf Coast | 978-1-7281-5446-6/20/$31.00 ©2020 IEEE | DOI: 10.1109/IEEECONF38699.2020.9389417

I. INTRODUCTION

High speed communication remains a very challenging task in underwater acoustic (UA) communications because of limited bandwidth, fast time variations of the channel, extended multi-path, refractive properties of medium, severe fading and large Doppler shifts [1]. Recently orthogonal frequency-division multiplexing (OFDM) has been adopted because of its remarkable capability in mitigating multipath interference with a low computational complexity [2, 3]. To improve the reliability of communication and boost data rate, adaptive modulation is used that involves the selection of transmission parameters according to the channel condition [4-8]. In non-adaptive (fixed) modulation, the transmitter does not exploit any information about the available channel parameters in choosing the modulation scheme. Alternatively, the channel information is made available to the transmitter in adaptive modulation and the performance of an adaptive modulation scheme depends on the transmitter's knowledge of the channel which is fed back from the receiver to the transmitter.

In this paper, multicarrier modulation is used in the form of OFDM and adaptive modulation and coding technique is considered in order to achieve high spectral efficiency in non-stationary UA environment. Signal-to-noise ratio (SNR) is estimated at the receiver and used as channel state information (CSI) to choose the adaptive allocation of the transmission parameters [7]. Then the transmitter sends this information back to the transmitter for the next data frame. Different modulation constellations are selected based on the SNR for the next data frame and thus higher data rate and better spectral efficiency can be achieved.

Adaptive modulation becomes challenging with the increase of Doppler frequency which leads to significant inter-carrier interference (ICI). ICI deteriorates the system performance resulting in low received SNR as it increases the power of received signal in the inactive (null) subcarriers and also misleads the detection of transmitted signal on active subcarriers. Thus the ICI affects the estimation of SNR, which in turn affects the performance of adaptive modulation. In this paper, null subcarriers are used to facilitate estimation of carrier frequency offset (CFO).

In this paper, a combination of National Instruments (NI) LabVIEW software and CompactDAQ device are adopted for real-time adaptive modulation for UA OFDM communication. The system design including both the transmitter and receiver is discussed. Compared to digital signal processor (DSP)-based design, the proposed implementation provides simplified integration with the hardware which helps rapid acquisition and visualization of data from NI input/output (I/O) or third-party I/O device, thus requiring less software development time [7, 8]. The performance of this real-time adaptive OFDM system is verified through a UA communication experiment conducted recently in a tank.

The rest of the paper is organised as follows. The system model is introduced in Section II. The channel model is presented in Section III. The adaptive modulation implementation is presented in Section IV. The real-time system implementation is described in Section V. The experiment results are discussed in Section VI. Conclusion is presented in Section VII.

II. SYSTEM MODEL

A frame-based coded UA OFDM communication system is considered in this paper. The frame structure of the transmitted signals is shown in Fig. 1. Each frame contains five OFDM data blocks and one preamble block. Each block contains pilot subcarriers, null subcarriers and data subcarriers. We assume that pilot subcarriers are uniformly spaced [9-11]. The preamble block is used for synchronization.

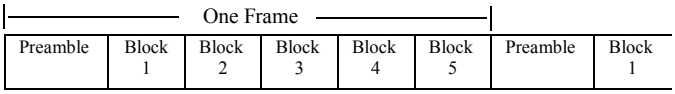

Fig. 1. Frame structure of the UA OFDM system.

In each frame, a binary source data stream $\boldsymbol{d} = (d[1], \dots, d[K_d])^T$ is generated, where $(\cdot)^T$ denotes the matrix (vector) transpose, K_d is the number of information-carrying bits in each frame. Each OFDM symbol is converted to the time domain by the inverse discrete Fourier transform (DFT), leading to the following baseband discrete time signal

$$\boldsymbol{x} = \boldsymbol{F}^H \boldsymbol{s} \tag{1}$$

where $(\cdot)^H$ denotes the conjugate transpose and $\boldsymbol{F}$ is a $K_s \times K_s$ DFT matrix. $\boldsymbol{s} = (s[1], \dots, s[K_s])^T$ is the OFDM symbol vector mapped from $\boldsymbol{d}$ depending on modulation constellations and K_s is the number of total subcarriers. The bandwidth of the transmitted signal is $B = f_{sc} K_s$, where f_{sc} is the subcarrier spacing. The duration of one OFDM symbol is $T = 1/f_{sc}$ and the total length of one OFDM block is $T_{total} = T + T_{cp}$, where T_{cp} is the length of cyclic prefix (CP). After removing the CP at the receiver end, the baseband discrete time samples of one OFDM symbol is

$$\boldsymbol{r}_t = \boldsymbol{P}\boldsymbol{F}^H \boldsymbol{S}\boldsymbol{F}\boldsymbol{h}_t + \boldsymbol{w}_t \tag{2}$$

where $\boldsymbol{S}$ = diag $(\boldsymbol{s})$ is a diagonal matrix and $\boldsymbol{w}_t = (w[1], \dots w[K_s])^T$ is the additive noise vector, $\boldsymbol{h}_t$ is the discrete time domain representation of the channel impulse response (CIR) and $\boldsymbol{P} = diag\ (1,\ e^{-j2\pi\epsilon/B}, \dots, e^{-j2\pi(K_s-1)\epsilon/B})^T$ is the phase distortion caused by the Doppler shift and ϵ is CFO.

After estimating and removing the frequency offset, the frequency domain representation of the received signal is

$$\boldsymbol{r}_f = \boldsymbol{S}\boldsymbol{h}_f + \boldsymbol{w}_f \tag{3}$$

where $\boldsymbol{w}_f$ is the additive noise vector in the frequency domain. $\boldsymbol{h}_f = (h_f[1], \dots . h_f[K_s])^T$ is a vector containing the channel frequency response (CFR) at all K_s subcarriers [11].

III. Channel Model

UA communication is challenging because of the unique channel characteristics of UA channel and considered as one of the most difficult communication channels due to the rapid dispersion in both time and frequency domain. UA channels are generally characterized by randomly time-varying multipath propagation which results in frequency selective fading. Additionally, motion of the transmitter and/or receiver introduces Doppler shift to the channel which contributes to the changes in CIR. The CIR can be defined as

$$h(\tau, t) = \sum_{p=1}^{N_p} h_p(t)\delta(\tau - \tau_p(t)) \tag{4}$$

where N_p is the number of propagation path, τ is delay, $\delta(.)$ is the Dirac delta function and t is the time at which the channel is observed. The coefficient $h_p(t)$ represents the gain of the pth path and $\tau_p(t)$ is the corresponding time-varying delay [12, 13].

A. CFO Estimation

In this paper, it is assumed that the motion of the transmitter and/or the receiver is causing the dominant Doppler shift. After removing CP from the received signal, CFO is estimated in null subcarriers in the receiver side. The CFO is performed in each OFDM block. The energy of the null subcarriers is used as the cost function.

$$J(\epsilon) = |\boldsymbol{\Theta}\boldsymbol{F}\boldsymbol{\Gamma}^H(\epsilon)\boldsymbol{r}_t|^2 \tag{5}$$

where $\boldsymbol{\Theta}$ is a selection matrix that picks the frequency-domain measurements on the null subcarriers out of all K_s subcarriers, $|\ |$ is the Euclidean norm of a vector, $\boldsymbol{\Gamma}(\epsilon) = diag\ (1,\ e^{j2\pi T_c \epsilon}, \dots, e^{j2\pi T_c (K_s-1)\epsilon})$ is diagonal matrix where $T_c = 1/B$ is the time interval for each sample. An estimation of ϵ is found through

$$\hat{\epsilon} = argmin\, J(\epsilon) \tag{6}$$

which is solved via 1-D search for ϵ [14].

Doppler shift is a constraint in UA communication which leads to ICI because signal components from one subcarrier spill over to the immediate neighbouring subcarriers. With the increase of Doppler frequency, the ICI increases the power of the received signal on inactive subcarriers. As a result the possibility of erroneous detection of subcarriers state enhances and in turn misleads the detection of transmitted symbols on the active subcarriers.

IV. Adaptive Modulation

Following the OFDM signal design, noise and received signal power is estimated in the frequency domain at the receiver. Received power at null subcarriers is used for noise variance estimation.

$$\hat{\sigma}_n^2 = \frac{1}{\bar{\mathcal{K}}_n} \sum_{m=1}^{\bar{\mathcal{K}}_n} \left| r_f[\mathcal{K}_n(m)] \right|^2 \tag{7}$$

where $\mathcal{K}_n$ is the set containing the indices of null subcarriers and for a set $\mathcal{X}$, $\bar{\mathcal{X}}$ denotes the number of elements in $\mathcal{X}$ and $r_f[m]$ is the frequency-domain received signal at the m th subcarrier. The SNR in the frequency domain can be estimated as

$$\bar{\gamma} = \frac{\frac{1}{\bar{\mathcal{K}}_a} \sum_{m=1}^{\bar{\mathcal{K}}_a} \left| r_f[\mathcal{K}_a(m)] \right|^2}{\frac{1}{\bar{\mathcal{K}}_n} \sum_{m=1}^{\bar{\mathcal{K}}_n} \left| r_f[\mathcal{K}_n(m)] \right|^2} - 1 \tag{8}$$

where $\mathcal{K}_a$ is the set containing the indices of pilot and data subcarriers, i.e., $\mathcal{K}_a = \mathcal{K}_p \cup \mathcal{K}_d$ [1]. The estimated SNR is used to choose the modulation mode adaptively. The chosen modulation mode is fed back to the transmitter for the next data frame. The received SNR is estimated in frequency domain after CFO estimation and compensation. The SNR estimation algorithm performs better at lower Doppler frequency than the higher Doppler frequency which is shown in [15]. We would like to note that the estimated received SNR reflects the effect of Doppler frequency.

The block diagram of the proposed adaptive modulation scheme in Fig. 2 shows that channel estimation and SNR estimation are done in the receiver side. After that the channel equalization is performed. Then a proper modulation mode is selected by the mode selector block depending on the estimated SNR for the next data frame. The selected modulation mode for

the next data frame is fed back to the transmitter. The adaptive modulator block at the transmitter side consists of different modulators which provide different modulation mode and modulate the data frame according to the selected mode. The demodulator block demodulates the received signal according to the selected modulation mode.

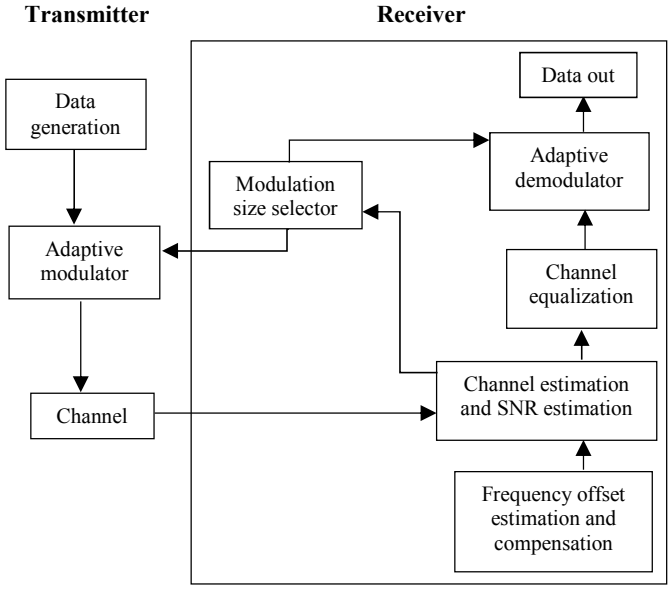

Fig. 2. Block diagram of adaptive modulation scheme.

In this work, the adaptation is done frame by frame. Individual modulation scheme results have been observed and analyzed for UA communication systems for fixed modulation. Extensive simulations of fixed modulation for different modulation schemes are used to select the target bit-error-rate (BER) and the estimated SNR is used as switching parameter [4, 7]. Switching threshold for adaptive modulation system is determined to keep the overall BER lower than the target BER. In fact, the highest modulation order is chosen under a certain BER and SNR. Therefore, a better tradeoff between data rate and overall BER is achieved by the proposed adaptation system. Switching thresholds used for the adaptive modulation schemes are presented in Table I.

TABLE I. SWITCHING THRESHOLD FOR ADAPTIVE MODULATION SCHEMES.

Mode	Modulation	Threshold
1	BPSK	SNR < 13.25 dB
2	QPSK	13.25 dB ≤ SNR ≤ 24.5 dB
3	16QAM	SNR > 24.5 dB

V. SYSTEM IMPLEMENTATION

A. System Hardware

An NI CompactDAQ data generation and acquisition system is adopted in our experiment which is capable of analog I/O, digital I/O, counter/timer operations, and industrial bus communication. It consists of a chassis and NI I/O modules. In the CompactDAQ system, an NI cDAQ-9174 plug-and-play chassis is connected to a laptop through USB where the NI LabVIEW software is installed for the signal generation, acquisition and processing. It is a four slot chassis which controls the timing, synchronization, and data transfer among up to four I/O modules and the external host (computer).

An NI-9260, 2-channel voltage output module and an NI-9232, 3-channel dynamic signal acquisition module are plugged into two of the four slots of the chassis for signal generation and acquisition respectively. The CTG0052 acoustic transducer is connected to the NI-9260 module through a transformer matching network and a power amplifier to transmit acoustic signals through the UA channel. The Reson reference and HTI-96-Min hydrophones are connected to the NI-9232 modules through preamplifiers to acquire signals received from the UA channel for the forward and feedback links respectively. For adaptive modulation two sets of devices are used. One set is designed for the forward link and the other set is designed for the feedback link.

TABLE II. PARAMETERS USED IN EXPERIMENT

Bandwidth	B = 4 kHz
Number of subcarriers	K_s = 512
Subcarrier spacing	f_{sc} = 7.8 Hz
Length of OFDM symbol	T = 128 ms
Length of CP	T_{cp} = 25 ms
Number of pilot subcarriers	K_p = 128
Number of data subcarriers	K_d = 325
Number of null subcarriers	K_n = 59

B. Software Implementation

The software of our adaptive UA OFDM system is designed and implemented using NI LabVIEW. The system parameters used in the experiment are listed in Table II. The system generates one frame and forwards the generated data frame to the channel 1 of NI 9260 (DAQ1/Slot2/channel1). The CTG0052 (1) transducer transmits the signal through the UA channel. Then the Reson reference hydrophone receives the signal and forwards the received data to NI9232 (DAQ2/Slot1/channel1). Then the signal is processed by the receiver in LabVIEW. At first, the signal samples received by NI9232 are converted from the passband to the baseband. The receiver first removes the CP from each OFDM block. Then the frequency offset estimation and compensation is performed for each OFDM symbol using the null subcarriers. Then the SNR is estimated in frequency domain. After that the baseband signals are passed through channel estimation. The least-squares (LS) method is used to estimate the frequency domain channel response at the pilot subcarriers. The estimated channel response is used to equalize the received signals. Demodulation operation is performed to the equalized signals.

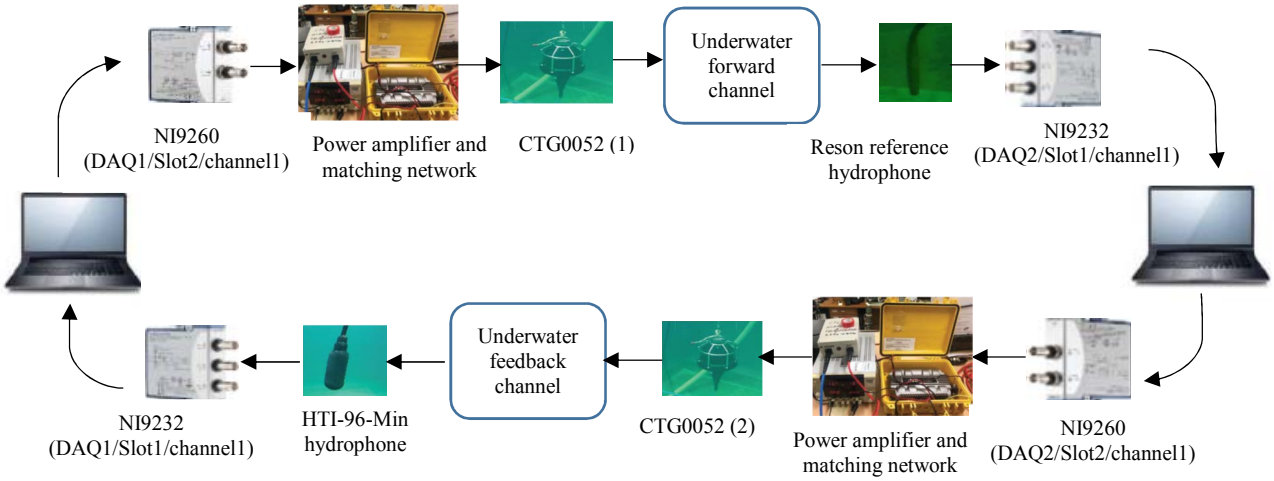

Fig. 3. LabVIEW-based implementation of real-time adaptive modulation for UA OFDM system.

After estimating the SNR of the received signal, the modulation size is selected depending on the channel condition for the next frame transmission. Data symbols containing the modulation size information are modulated by BPSK constellations and forwarded to NI-9260 (DAQ2/Slot2/channel 1). The CTG0052 (2) transducer feeds back the modulation size information signal through the UA feedback channel. The HTI-96-Min hydrophone receives the modulation size signal and forwards the received data to NI9232 (DAQ1/Slot1/channel1) for processing. The real-time adaptive modulation scheme is shown in Fig. 3.

VI. Experiment Results and Discussion

In the tank experiment, in order to obtain the SNR thresholds for various modulation schemes under a target BER, we first perform one-way communication experiment with a pair of transducer and hydrophone. The received SNR is changed through varying the power of the transmitted signal. After the SNR thresholds are obtained, the experiment of adaptive modulation is performed by placing another pair of transducer and hydrophone in the tank. Fig. 4 shows the location of the transducers and hydrophones in the tank during the experiment. The length, width and depth of the tank are 2.5 m, 1.5m and 1.8 m respectively.

Fig. 4. Location of the transducers and hydrophones for forward and feedback links.

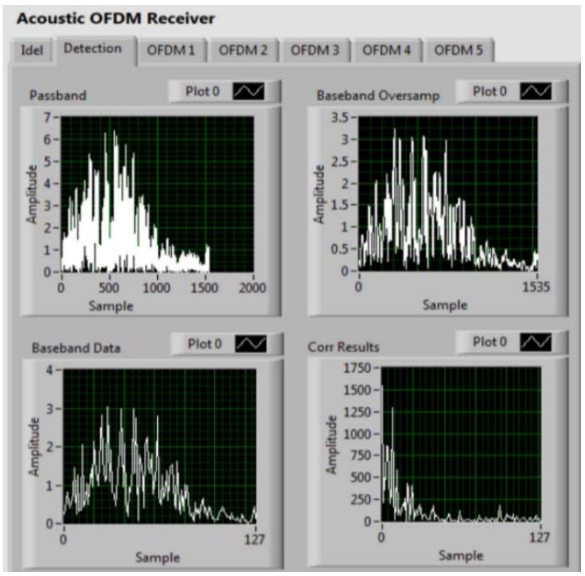

Fig. 5. Received data frame in acoustic OFDM receiver during the tank experiment.

During the experiment, we bypassed the frequency offset estimation and compensation module in Fig. 2 as the Doppler shift is very small in a tank.One successfully detected data frame and magnitude of the cross-correlation between the received synchronization sequence and local synchronization sequence are shown in Fig. 5. The peak position represents the position of the strongest channel path while other non-negligible local peak values represent the other channel path positions which means that there are multiple paths between the transmitter and receiver because of the reflections of acoustic signals in the wall of the tank. The power of the CIR estimated by the pilot subcarriers is shown in Fig. 6. It can be seen that the maximum channel delay spread is 15 ms which is shorter than the CP length.

Fig. 7 shows the results of the adaptive modulation for UA OFDM system performed in the tank. The first OFDM frame transmits with the BPSK constellations (indicated by "1" in the top ModSize box in Fig. 7(a)) and the received symbols are

correctly aggregated into the BPSK constellations after the channel equalization. As the received SNR is within the thresholds of the QPSK modulation in Table I, the modulation size is selected to QPSK (as indicated by "2" in the lower Mod Size box in Fig. 7(a)) in the receiver side and fed back to transmitter for the next transmission. Then the received symbols of the next frame are correctly aggregated into the QPSK constellations. As we further increase the transmit signal power, the received SNR is above the threshold of the 16QAM modulation in Table I. Thus, the receiver feeds back this modulation scheme (indicated by "4" in the lower Mod Size box in Fig. 7(b)).

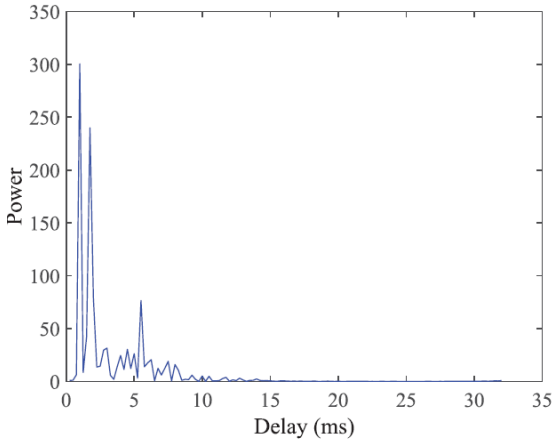

Fig. 6. Estimated power of the CIR during tank experiment.

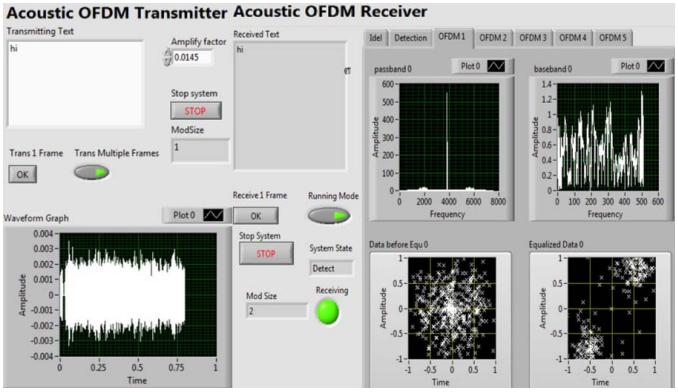

(a)

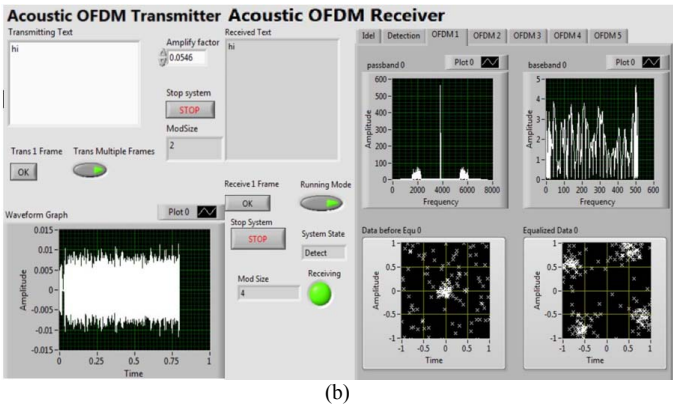

(b)

Fig. 7. Adaptive modulation for UA OFDM system in the tank.

The BER vs SNR results are shown in Fig. 8 for fixed (BPSK, QPSK and 16QAM) and adaptive modulation schemes. The target uncoded BER in this experiment is determined as 0.1. Switching thresholds for the adaptive modulation scheme are determined using the BER results of the fixed modulation schemes in Fig. 8 and presented in Table 1 to keep the overall BER lower than 0.1. In fact, the highest modulation order is chosen under a certain BER and SNR. Therefore, a better tradeoff between data rate and overall BER can be achieved by the proposed adaptation system.

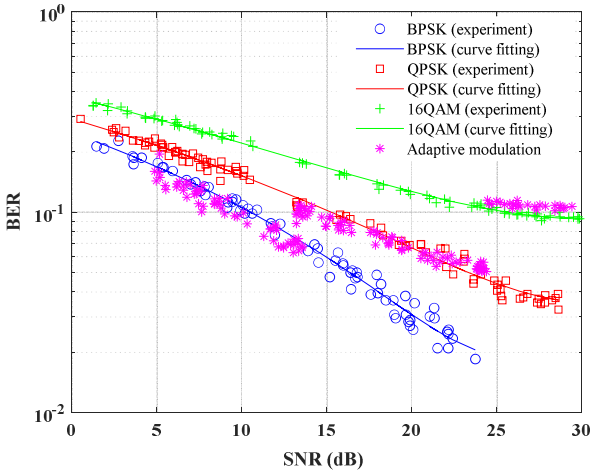

Fig. 8. BER performance of the proposed adaptive modulation schemes in tank experiment.

VII. Conclusion

A LabVIEW based adaptive modulation scheme for UA OFDM communication system is proposed in this paper. The performance results of the proposed scheme in the tank are presented. SNR is chosen as performance metric for mode switching which also reflects the effect of ICI. The adaptive scheme depends on the estimated SNR of the previous frame to choose adaptive allocation of the modulation size for the next frame. The proposed adaptive system can ensure higher data rate at the target BER compared to fixed modulation.

Acknowledgment

This research is supported by an Australian Government Research Training Program (RTP) Stipend and RTP Fee-Offset Scholarship through Curtin University. We also want to thank CMST, Curtin for providing support for tank experiment.

References

[1] S. Zhou and Z. Wang, "OFDM for underwater acoustic communications", John Wiley & Sons, Ltd, 2014.

[2] P. Chen, Y. Rong, S. Nordholm, Z. He, and A. Duncan, "Joint channel estimation and impulsive noise mitigation in underwater acoustic OFDM communication systems," IEEE Trans. Wireless Commun., vol. 16, pp. 6165-6178, Sep. 2017.

[3] P. Chen, Y. Rong, S. Nordholm, and Z. He, "Joint channel and impulsive noise estimation in underwater acoustic OFDM systems," IEEE Trans. Veh. Technol., vol. 66, pp. 10567-10571, Nov. 2017.

[4] L. Wan, H. Zhou, X. Xu, Y. Huang, S. Zhou, Z. Shi and J.H. Cui, "Adaptive modulation and coding for underwater acoustic OFDM", IEEE J. of Oceanic Engineering, vol. 40, no. 2, pp. 327-336, Apr. 2015.

[5] S. Xiaohong, W. Haiyan, Z. Yuzhi and Z. Ruiqin, "Adaptive Technique for Underwater Acoustic Communication", IntechOpen Journal, 2012.

[6] A. Radosevic, R. Ahmed, T. Duman, J. Proakis and M. Stojanovic, "Adaptive OFDM modulation for underwater acoustic communications: Design considerations and experimental results", IEEE J. of Oceanic Engineering, vol. 39, no. 2, Apr. 2014.

[7] K. Pelekanakis, L. Cazzanti, G. Zappa and J. Alves, "Decision tree-based adaptive modulation for underwater acoustic communications", 2016 IEEE Third Underwater Communications and Networking Conference (UComms), Lerici, pp. 1-5, 30 Aug.-1 Sept. 2016.

[8] M. Sadeghi, M. Elamassie and M. Uysal, "Adaptive OFDM-based acoustic underwater transmission: System design and experimental verification," IEEE International Black Sea Conference on Communications and Networking, Istanbul, pp. 1-5, 2017.

[9] P. Chen, Y. Rong, S. Nordholm, A. Duncan and Z. He, "A LabVIEW based implementation of real-time underwater acoustic OFDM system", 23rd Asia-Pacific Conference on Communications, pp. 1-5, Dec. 2017.

[10] P. Chen, Y. Rong, S. Nordholm, and Z. He, "An underwater acoustic OFDM system based on NI CompactDAQ and LabVIEW," IEEE Systems Journal, vol. 13, pp. 3858-3868, Dec. 2019.

[11] P. Chen, Y. Rong, and S. Nordholm, "Pilot-subcarrier based impulsive noise mitigation for underwater acoustic OFDM systems," in Proc. WUWNet, 2016, Shanghai, China, Oct. 2016.

[12] M. Stojanovic and J. Preisig, "Underwater acoustic communication channels: Propagation models and statistical characterization", IEEE Communications Magazine, vol. 47, no. 1, pp. 84-89, Jan. 2009.

[13] A. Radosevic, T. M. Duman, J. G. Proakis and M. Stojanovic, "Channel prediction for adaptive modulation in underwater acoustic communications," OCEANS 2011 IEEE, Spain, Santander, pp. 1-5, 2011.

[14] M. Huang, S. Sun, E. Cheng, X. Kuai and X. Xu, "Joint interference mitigation with channel estimated in underwater acoustic OFDM system", TELKOMNIKA, vol. 11, no. 12, pp. 7423-7430, 2013.

[15] S. Barua, Y. Rong, S. Nordholm and P. Chen, "Adaptive Modulation for Underwater Acoustic OFDM Communication", Proc. MTS/IEEE OCEANS, Marseille, France, June 17-20, 2019.